



Published in final edited form as:

*Science*. 2021 April 09; 372(6538): 150–156. doi:10.1126/science.abe7790.

## Bilateral visual projections exist in non-teleost bony fish and predate the emergence of tetrapods

Robin J. Vigouroux<sup>1</sup>, Karine Duroure<sup>1</sup>, Juliette Vouigny<sup>2</sup>, Shahad Albadri<sup>1</sup>, Peter Kozulin<sup>3</sup>, Eloisa Herrera<sup>4</sup>, Kim Nguyen-Ba-Charvet<sup>1</sup>, Ingo Braasch<sup>5</sup>, Rodrigo Suárez<sup>3</sup>, Filippo Del Bene<sup>1,\*</sup>, Alain Chédotal<sup>1,\*</sup>

<sup>1</sup>Sorbonne Université, INSERM, CNRS, Institut de la Vision, 17 Rue Moreau, 75012 Paris, France

<sup>2</sup>Institut Curie, PSL Research University, INSERM U934, CNRS UMR3215, Paris, France

<sup>3</sup>Queensland Brain Institute, The University of Queensland, Building 79, St Lucia Campus, Brisbane, QLD 4072, Australia

<sup>4</sup>Instituto de Neurociencias Av. Ramón y Cajal s/n San Juan de Alicante 03550 Spain

<sup>5</sup>Department of Integrative Biology and Program in Ecology, Evolution and Behavior, Michigan State University, 288 Farm Lane, East Lansing MI 48824, USA

### Abstract

In most vertebrates, camera-style eyes contain retinal ganglion cell neurons projecting to visual centers on both sides of the brain. However, in fish, ganglion cells are thought to only innervate the contralateral side. This suggested that bilateral visual projections appeared in tetrapods. Here, we show that bilateral visual projections exist in non-teleost fishes and that the appearance of ipsilateral projections does not correlate with terrestrial transition or predatory behavior. We also report that the developmental program specifying visual system laterality differs between fishes and mammals as the *Zic2* transcription factor which specifies ipsilateral retinal ganglion cells in tetrapods appears absent from fish ganglion cells. However, overexpressing human *ZIC2* induces ipsilateral visual projections in zebrafish. Therefore, the existence of bilateral visual projections likely preceded the emergence of binocular vision in tetrapods.

### One sentence summary:

Bilateral vision preceded terrestrial life

---

Eye position on the head is highly variable between species, but frontal eyes have long been considered critical for depth perception (stereopsis) by increasing the overlap of the right and left eye visual fields (1). In vertebrates, ganglion cell axons from each eye cross through each other at the optic chiasm and enter the brain on the contralateral side. In

---

\*Corresponding authors. filippo.delbene@inserm.fr and alain.chedotal@inserm.fr.

**Authors contribution:** AC, FDB and RV designed the experiments. FDB, KD, KNBC, JV, SA, RV, PK, RS conducted the experiments. AC, KNBC and FDB obtained funding for the project. IB provided *Lepisosteus* samples and EH the human *ZIC2* cDNA. AC, FDB and RV designed the figures and wrote the manuscript. All authors discussed the results and commented on the manuscript.

**Competing interests:** The authors declare no competing interests.

mammals, visual axons from each eye meet and interweave at the chiasm. However, optic nerve crossing modalities are more diverse in fish and in most species the two optic nerves remain fully separated and only overlap at the chiasm (2, 3).

Classic neuroanatomical studies showed that in mammals, eye projections are bilateral with a variable fraction of retinal ganglion cell (referred to as ganglion cell thereafter) axons continuing in the ipsilateral optic tract after crossing the chiasm. The proportion of ipsilateral projections is low (2-3%) in rodents but reaches around 40% in primates (4, 5). The comparative analysis of many vertebrate species conducted over several decades suggests that ipsilateral visual axons exist in all mammals, anuran amphibians, some reptiles, and that they are essentially absent or were secondarily lost in birds (5–8). Accordingly, developmental transcriptional programs specifying ipsilateral ganglion cells described in mammals are conserved in *Xenopus* but not in chick and zebrafish (5, 9). This textbook view implies that visual axon bilaterality emerged in early tetrapods and might have provided a visual advantage, in particular for nocturnal and predatory terrestrial species (10). However, a review of the extensive literature on fish visual systems gives a more complex image with reports, sometimes contradictory, of ipsilateral ganglion cell projections in some fish species (6, 11). Most of these pioneering studies relied on imprecise histological staining methods such as the Nauta-Gygax staining method or autoradiography (12). Here, we assessed the laterality of visual projections in bony fishes (Fig. 1A) with the B fragment of the cholera toxin (12) coupled to fluorescent dyes. Dye-coupled Cholera toxins have not been previously used in fish although they proved to be highly reliable tracers for visual projections in rodents due to their efficient endocytosis by neurons, slow elimination, high photostability and brightness (13). They are also compatible with whole-brain clearing and thereby allow mapping visual pathways in intact brain using 3D light sheet fluorescence microscopy (14, 15).

With more than 30,000 species, fishes account for at least half of the extant vertebrate species (16). We initially focused on ray-finned fishes (Actinopterygians; Fig. 1A and fig. S1) which separated from lobe-finned fish (Sarcopterygians, including tetrapods) around 450 Million years ago (Ma)(17). Within ray-finned fishes, we initially selected 6 species among the clupeocephalan lineage (fig. S1), the largest of the three lineages of teleost fishes which account for most (about 96%) of extant teleosts (18). Within clupeocephalans, three represent ostariophysians (Mexican tetra *Astyanax mexicanus*, redeye piranha *Serrasalmus rhombeus*, and zebrafish *Danio rerio*) and three are percomorphs (green-spotted pufferfish *Tetraodon nigroviridis*, Atlantic mudskipper *Periophthalmus barbarus*, and four-eyed fish *Anableps anableps*). With 9,000 and 16,000 species respectively, ostariophysians and percomorphs are the two largest clades of teleosts. They have diverse eye positions, feeding behaviors, and habitats and some were previously reported to have ipsilateral visual projections (11).

## Totally crossed visual projections in teleosts

The visual system of the zebrafish has been extensively studied using lipophilic dye tracing or genetic methods and shown to be exclusively contralateral (19). Accordingly, we found that fluorescent (Cholera toxin labelled) axons were only present on the contralateral side

of adult zebrafish brains (Fig. 1B and movie S1; n=6). Previously identified retino-recipient visual nuclei (20) could be detected with cholera toxin, thereby validating the use of this tracing method in fish (Fig. 1C). Light-sheet microscopy imaging of cholera toxin injected fish, showed that visual projections were only contralateral in Mexican tetra surface fish (Fig. 1, D and E and movie S1; n=7), contradicting a previous study (21). Likewise, eyes in the redeye piranha only projected contralaterally (Fig. 1, F and G and movie S1; n=3), in disagreement with earlier work in other piranha species (22, 23). This suggests that ostariophysians only have crossed visual projections.

In the fresh water green-spotted pufferfish (24), a percomorph, the 2 optic nerves stay separated at the chiasm and visual projections were exclusively contralateral (Fig. 1, H and I and fig. S2 and movie S1; n= 4) as previously described in another pufferfish (25). We next studied the four-eyed fish, a percomorph surface dweller fish whose large protruding eyes with duplicated corneas and pupils allows seeing under and above the water (26). Again, one optic nerve passed over the other at the chiasm (fig. S2) and cholera toxin tracing showed that in this species, visual projections were also completely crossed (Fig. 1, J and K; n= 3). Similar results were obtained in the mudskipper, a percomorph with amphibious lifestyle (Fig. 1, L and M and fig. S2 and movie S1; n= 3). Together, these results show that in percomorph eyes, ganglion cells also likely only project to visual nuclei on the opposite side of the brain (fig. S1).

Osteoglossomorphs (bonytongues), a teleost sister groups of clupeocephalans (Fig. 1A and fig. S1), are considered a group of basal (i.e the group which gave rise to later forms) teleosts constituted of about 200 living species (16). We chose to trace visual projections in the African butterflyfish (*Pantodon buchholzi*), a predator living close to the surface of freshwater system, and found a small contingent of retinal axons (Fig. 2, A and B and movie S1,  $2.33\pm 0.23$  % ipsilateral projections in the optic tectum; n=3) project to the ipsilateral side, corroborating an earlier report (27). The main portion of ipsilateral axons targeted the tectum and some others targeted pretectal nuclei. Ipsilateral visual axons have also been described in a mormyrid electric fish (*Gnathonemus petersii*) (28), another osteoglossomorph with a more nocturnal predatory behavior that can orient by active electrolocation (29). These results show that bilateral visual projections exist in osteoglossomorph teleosts regardless of their predatory strategy and lifestyle history. Therefore, within teleosts, ipsilateral projections could have been secondarily lost in clupeocephalans or independently acquired in osteoglossomorphs. In mammals, binocular inputs to visual targets/areas are either segregated (thalamus, colliculus) or intermingled (suprachiasmatic nucleus). As both eyes were injected with 2 distinct Alexa-conjugated-cholera toxins, we also studied the relative distribution of ipsilateral and contralateral ganglion cell axons in butterflyfish brain areas innervated by both eyes. This showed that in African butterflyfish (Fig. 2C) retinal inputs from both sides segregated, as in the thalamus and superior colliculus of mammals.

### **Bilateral visual projections exist in basal ray-finned fishes**

These results on teleosts led us to study retinal projections in non-teleost ray-finned fish lineages (Holosteans, Acipenseriforms, and Polypteriforms, Fig. 1A) which split from

teleosts before the teleost whole genome duplication event (TGD, Fig. 1A) that occurred around 320 Ma in the ancestor of extant teleosts (reviewed in (30)). Holosteans and Acipenseriforms are considered to have evolved slowly since they branched from other vertebrates 350 Ma (31). Bilateral visual projections (movie S2, n=5/5) were observed in the spotted gar (*Lepisosteus oculatus*), one of the seven extant species of garfish, and a representative of the holosteans. The spotted gar is a unique vertebrate model system as its genome is thought to provide a “bridge” between tetrapods and teleosts (32). Bilateral cholera toxin injections revealed an ipsilateral projection in the rostral optic tectum of the spotted gar, with visual axons targeting several pretectal nuclei. There was no overlap of the contralateral and ipsilateral axons (Fig. 2, D to F and movie S2, n=5/5) which represented  $4.78 \pm 0.46$  % of visual inputs in the tectum, a ratio comparable to rodents. Next, we traced visual projections in the acipenseriform sterlet sturgeon (*Acipenser ruthenus*, n=2/2). Cholera toxin tracing demonstrated the existence of a binocular domain in the tectum of the sterlet sturgeon as well as in several pretectal nuclei (Fig. 2, G to J and movie S2;  $9.77 \pm 1.28$  % ipsilateral projections in the tectum, n=2). No re-crossing of visual inputs after entering the brain were detected contrary to previous observations in the Russian sturgeon *Acipenser güldenstädtii* (33). We then studied the armored bichir (*Polypterus delhezi*, n=2/2), a carnivorous nocturnal fish representing the most basally diverging lineage of extant ray-finned fishes, the Polypteriforms. In the bichir, the two optic nerves meet at the chiasm and ganglion cells axons interweave during decussation (fig. S2). Ipsilateral axons projected to numerous pretectal nuclei such as the nucleus opticus dorsolateralis anterior thalami, the area optica ventrolateralis thalami, and the nucleus commissurae posterior par magnocellularis (Fig. 2, K to N and movie S2). This corroborates previous studies in gray bichir *Polypterus senegalus* (34). These results, together with similar observations in the holosteans longnose gar (*Lepisosteus osseus*) and the bowfin (*Amia calva*) (35, 36) indicate that bilateral visual projections likely are ancestral among actinopterygians and arose before their diversification and that the ipsilateral component likely was subsequently lost in clupecocephalans. To further test this hypothesis, we analyzed visual projections in the Australian lungfish (*Neoceratodus forsteri*) a basal member of the lobe-finned fishes (Sarcopterygians) the monophyletic group that includes tetrapods. Lobe-finned fishes diverged from ray-finned fishes about 450 Ma and lungfish are now considered the closest living fish relative of tetrapods (17). In all injected animals (n=6/6) a small ipsilateral projection was found innervating the optic tectum (Fig. 2, O to S and movie S3, n=6). In contrast to other fish species analyzed here, ipsilateral projections intermingled with contralateral ones (Fig. 2, R and S; n=6). This was consistent with an earlier analysis of a single specimen of Australian lungfish (37) and supports the existence of bilateral visual projections in the bony vertebrate ancestor of actinopterygians and sarcopterygians (fig.S1). This intermingling of ipsilateral and contralateral axons could have some functional implications as it suggests that some tectal neurons might receive and integrate inputs from both eyes. Alternatively, it could represent an immature stage of visual system development that could be resolved in adult animals in an activity-dependent manner as it is the case in mammals. Together, these results indicate that the bilateral organization of the visual system likely did not appear in amniotes but that it is an ancestral vertebrate feature that emerged much earlier in evolution, before water-to-land transition and aerial vision adaptation in tetrapods.

## Zic2 expression in the ipsilateral human embryonic retina

Our results raised questions about the evolution and conservation of the genetic mechanisms underlying visual system binocularity. Are they conserved in ray-finned fish with bilateral visual projections? The zinc-finger transcription factor Zic2 specifies the ipsilateral identity of ganglion cells in developing mice, ferrets and *Xenopus* (5). In *Xenopus*, Zic2 is absent from the neural retina of pre-metamorphic tadpoles that have only crossed visual projections, but Zic2 is expressed in ipsilaterally projecting ganglion cells after metamorphosis (5). To further evaluate and support the implication of Zic2 in the control of mammalian ganglion cell laterality, we analyzed the expression of ZIC2 in the human eye and compared it to mice by performing immunohistochemistry in whole-mount retinas. In human embryos, ganglion cell axons reach the brain by the 7th post-conception week (pcw7) and the optic nerve is well formed at pcw10 (38). Using the EyeDISCO clearing protocol (15) in mice, we observed that at embryonic day 16 (E16), the peak of Zic2 expression in mice (5), the retinal domain positive for Zic2 represented about  $5.34 \pm 0.36$  % of the total retinal surface (Fig. 3, A to C and fig. S3A; n=6 eyes). Post-mitotic ganglion cells, the first neurons generated in the retina(39), migrate to the basal side to accumulate at the inner surface of the retina and express the transcription factors Islet1 (40) and RNA-binding protein with multiple splicing (RBPMS)(41) (Fig. 3). At pcw9, RBPMS+ and ISLET1+ ganglion cells were present all over the retina (Fig. 3, D to I). Flat-mounted and sections of human retinas from pcw9 embryos, an age equivalent to E16 in mice (40), showed that ZIC2+ cells were restricted to the temporal quadrant of the retina (representing about  $18.95 \pm 0.98$  % of the retina surface), which contains ipsilaterally projecting ganglion cells in primates (Fig. 3, D to J and movie S4; n=3 eyes). ZIC2+ were ganglion cells as they co-expressed ISLET1 and RBPMS (Fig. 3, F to H). In the temporal retina, the density of ZIC2+/ISLET1+ ganglion cells was higher close to the ciliary marginal zone, at the edge of the retina (Fig. 3G), than in more medial regions where it was absent from the most superficial ISLET1+ (Fig. 3H and fig. S3B) and RBPMS+ ganglion cells (Fig. 3F and fig. S3). ZIC2 was not detectable in the nasal retina (Fig.3, D, E and I). Unlike in the mouse (42), ZIC2 was not present in the neuroblastic layer which contains SOX2 (sex determining region Y-box 2) + progenitors (Fig. 3, J to L and fig. S3C). At pcw14, at the end of ganglion cell neurogenesis (39), ZIC2 was still only present in the temporal retina (Fig. 3, K and L). Although we could not access later stages of development, the absence of ZIC2 from the most superficial ganglion cells in the inner retina suggest that human ZIC2 is expressed in recently differentiated ipsilateral ganglion cells in the temporal retina and might be down-regulated as they mature, as is the case in mice.

## Zic2 is not expressed in differentiating ganglion cells in fish with bilateral visual projections

The pivotal role for Zic2 in the specification of an ipsilateral axonal growth program in mammals was also well correlated with the absence of transcripts of the two *zic2* co-orthologs (*zic2a* and *zic2b*, generated in the TGD) in zebrafish ganglion cells (43) (fig. S4, A to C and E to G). Double fluorescent *in situ* hybridization for *zic2b* and *atoh7* (a committed precursor marker) from 24 to 48 hours post fertilization confirmed that *zic2b* did not colocalize with differentiating *atoh7*+ ganglion cells. By contrast, and as reported for *zic2* in the mouse (44), *zic2b* was detected in the ciliary marginal zone, (fig. S4M, n=3)

which contains dividing progenitors and stem cells producing all retinal cell types, even in adult teleosts (45, 46) (fig. S4, H to L; n=5).

The presence of an ipsilateral visual projection in the spotted gar, as extensive as that of mice, together with its well characterized genome and the accessibility of gar embryos (32, 47), led us to evaluate the expression of *zic2* in the developing gar retina. We first analyzed the development of the gar visual system using whole-mount immunolabelling, iDISCO+ clearing and light-sheet microscopy (Table S1) (15). In the spotted gar, a few Islet1- immunoreactive ganglion cells were detected at 2-3 days post fertilization (dpf) (Fig. 4, A and B and fig.S5C and movie S5; n=5). At 6-7dpf, optic nerves could be observed and had reached the optic chiasm (Fig. 4, C and D and movie S5; n=5). Development is slower in gar than in zebrafish and it is temperature-dependent (48). The next 10 days of development are only characterized by changes in fin opercular and gill formation but not in eye morphogenesis (48). By 17-18dpf the retina contained many ganglion cells and the optic tract was well developed (Fig. 4, E to G and movie S5; n=5). The highly proliferative ciliary marginal zone could be identified by the presence of cells expressing the S-phase marker, proliferating cell nuclear antigen marker and overlapping with *zic2* expression, which was absent from neighboring post-mitotic Islet1+ ganglion cells (Fig. 4, H to L). At 2-3dpf and 6-7 dpf, *zic2* mRNA was detected in proliferating cells of the developing neuroretina and progressively became restricted to the ciliary marginal zone (fig. S5, A to D). Its paralogs, *zic1* and *zic5*, also enriched in ipsilateral ganglion cell in mice (49), were absent from the embryonic gar retina (fig. S5, E to L). These results show that neither *Zic2*, *Zic1* nor *Zic5*, specify ipsilateral ganglion cells in the spotted gar, suggesting that *zic* genes might be dispensable for gar ipsilateral projections. By contrast, the presence of *Zic2* in the ciliary marginal zone of fish and mammals suggests that *Zic2* might have a function in retinal precursors that is evolutionarily conserved.

In mammals, *Zic2* acts in part by activating the expression of the receptor tyrosine kinase EphB1 in ipsilateral axons (8, 50), whose ligand ephrinB2, localized at the chiasm, prevents crossing (7). According to the lack of *Zic2* in the gar ganglion cells, we did not detect *ephB1* mRNA in the developing retina and *ephrinB2* was absent from the chiasm (fig. S5, M to W).

### **Zic2 overexpression induces ipsilateral projections in zebrafish**

In mice, *Zic2* overexpression in the retina, outside the ipsilateral domain, increases the proportion of ipsilaterally projecting ganglion cell axons (50). Therefore, we tested the hypothesis that despite its absence in fish ganglion cells, the forced expression of *Zic2* in zebrafish ganglion cells could affect their axonal targeting. We used a human *ZIC2-T2A-GFP* overexpression construct to express *ZIC2* and GFP in the zebrafish eye under the control of the *atoh7* promoter. Vertebrate *Zic2* proteins are highly conserved (51), with 81.1% identity between Human *ZIC2* and zebrafish *Zic2a* and more than 93% similarity in the zinc finger domain (fig. S6). To visualize the projections coming from *ZIC2* overexpressing ganglion cells derived from a single eye, we removed one eye at 2 dpf. As previously reported, under normal conditions retinal fibers from the remaining eye projected exclusively to the contralateral tectum (Fig. 4, M and N; n=10) (52, 53). In contrast, *ZIC2*-expressing ganglion cells generated ipsilateral retinotectal afferent fibers representing



a mean of  $19.6 \pm 8.5\%$  of the GFP+ axons (Fig. 4, O and P;  $n=10/13$ ). Expression of *ZIC2* did not seem to bias the targeting of ganglion cell axons to their topographic position as previously reported in mouse (54). These results show that *zic2*, although not normally expressed in zebrafish ganglion cells, can still specify an ipsilateral program. In mice, the receptor tyrosine kinase EphB1 is expressed by ipsilateral ganglion cell axons and the ectopic expression of *Zic2* in the contralateral retina induces EphB1 and reduce midline crossing at the chiasm (8, 50). However, we could not detect EphB1 protein or mRNA (fig. S7) in zebrafish ganglion cells, neither in controls injected with GFP ( $n=13$ ) nor in *ZIC2*-overexpressing fish ( $n=11$ ) suggesting that these may be guided by alternative cues.

## Discussion

It has been proposed that the evolution of terrestrial vertebrates followed an increase of eye size in aquatic vertebrates able to see through air, in a process that has occurred also in modern crocodiles or fish species similar to the four-eye fish and mudskippers (55). The existence of ipsilateral projections in the most basally branching groups of both actinopterygians and sarcopterygians indicates that ipsilateral connections were likely already present in the common ancestor of bony vertebrates, a bony fish, thus preceding aerial vision adaptation of tetrapods. This example highlights how the comparative study of a variety of species outside the list of the classical model species allows drawing evolutionary conclusions that may otherwise remain obscured (56). Moreover, all the teleosts species analyzed in our study can be described as diurnal predators that heavily rely on visual cues to detect and consume their preys. These preys may vary in size from large vertebrates (redeye piranha) to small invertebrates (Mexican tetra, zebrafish, green-spotted puffer, Atlantic mudskipper and the four-eyed fish). In all cases our data show that ipsilateral projections in teleosts are not required for a visually mediated predatory behavior as it is usually assumed in mammals. Recent studies have confirmed this also in larval zebrafish where possible alternative neuronal circuits have been described (53).

On the other hand, lungfish and some basally branching actinopterygians, where ipsilateral projections are present, show reduced visual system development, as they are bottom dwellers that show nocturnal predatory behavior (lungfish and bichir) or feed on benthic organisms (sturgeon). Overall, our data show that the presence of ipsilateral projections in the visual system of fishes appears to correlate with phylogeny and not with life style or predatory behavior. Along these lines, it is therefore unlikely that ipsilateral retinal projections serve a function similar to what is commonly considered in mammals. On the contrary, visual system bilaterality might have been used as the neural substrate to compute stereopsis following the acquisition in diurnal mammals of visual-based predatory abilities after the Cretaceous–Paleogene (K–Pg) extinction event. Supporting this view, the number of ipsilateral projections in reptiles (chelonians and squamates) correlates neither with eye position nor with the degree of binocular field (11, 57). It has been hypothesized that ipsilateral ganglion cells facilitate motor coordination by providing a direct visual feedback to the limb steering brain centers (6). However, the function of ipsilateral ganglion cells in fish remains elusive and behavioral studies in non-canonical model species such as the gar will be required to address this question.

The conservation of the main families of axon guidance cues and receptors in Bilateria suggested that the mechanisms underlying the development of neuronal connectivity are evolutionarily conserved (58, 59). However, the loss of the gene encoding Deleted in Colorectal Cancer receptor in some bird species (60) and the uniqueness of the Roundabout3 receptor in mammals (61) have challenged this view. Here we show that the guidance program specifying visual axon ipsilaterality does not appear to be entirely conserved as we failed to detect expression of a *zic2* and other *zic* genes or *ephB1* in spotted gar ganglion cells. Hence, the textbook model of Zic2 and EphB1 in orchestrating retinal ganglion cell laterality does not simply translate to fish. In rodents, the contralateral identity of ganglion cells is specified by *Islet2* (62) and *SoxC* (63) transcription factors but whether they influence the development of visual axons in fish is unknown. Therefore, further experiments are needed to address the molecular mechanisms underlying visual bilaterality in bony fish species. Are there other pathways, apart from Zic2, that could direct ipsilateral projections or which could block the contralateral fate that occurs normally? A recent study (64) shows that in mice, contralateral ganglion cells activate a non-canonical Wnt signaling pathway to cross the midline. In ipsilateral ganglion cells, Zic2 prevents midline crossing by inducing a genetic module that changes the expression of a set of genes to jointly inhibit this non-canonical Wnt pathway.

In fact, the ectopic expression of human ZIC2 in the developing zebrafish retina still induces the formation of ipsilateral visual axons without causing other targeting defects. This finding suggests a possible conservation in fishes of downstream components of the genetic program specifying ipsilateral axons in mammals although the factor initiating its expression and its relationship to Zic2 remains unclear in the gar and in other non-teleost fish. By parsimony principle, given our data, we propose that the presence of ipsilaterality in the bony vertebrate ancestor is the most likely explanation. In particular, the Australian lungfish data show that ipsilateral projections were likely present in the sarcopterygian fish ancestor of tetrapods. Lungfish also functions as outgroup to the actinopterygians and thereby making an independent origin of ipsilateral visual axons within actinopterygians a less likely hypothesis. An alternative, yet less parsimonious explanation, could be that ipsilaterality has evolved independently multiple times among bony vertebrates, using different genetic mechanisms.

## Supplementary Material

Refer to Web version on PubMed Central for supplementary material.

## Acknowledgements

The authors wish to thank Anais Favre and Ali Abjaghrou for assistance with light-sheet microscopy, Fabio Cortesi for help with lungfish experiments, Sylvie Dufour and all members of Alain Chédotal and Del Bene teams for helpful discussions and input during the project. We thank Sylvie Rétaux (Paris Saclay University) for help with Mexican tetra work and helpful comments on the manuscript. We thank Allyse Ferrara and Solomon David (Nicholls State University) and members of the Braasch Lab for help with gar work.

## Funding:

Programme Investissements d'Avenir IHU FOReSIGHT (ANR-18-IAHU-01) (AC, FDB). INSERM cross-cutting program HuDeCA 2018 (AC). NIH R01OD011116 (IB). UQ Amplify Fellowship (RS).



## Data and materials availability:

All data are available in the manuscript or the supplementary materials.

## References

1. Ramón y Cajal S, *Histologie du système nerveux de l'homme & des vertébrés* (Maloine, Paris, 1909).
2. Walls GL, *The vertebrate eye and its daptative radiation* (Hafner Publishing company, Bloomfield Hills Michigan, 1942).
3. Mogi K et al. , Optic chiasm in the species of order Clupeiformes, family Clupeidae: Optic chiasm of *Spratelloides gracilis* shows an opposite laterality to that of *Etrumeus teres*. *Laterality*. 14, 495–514 (2009). [PubMed: 19229672]
4. Jeffery G, Erskine L, Variations in the architecture and development of the vertebrate optic chiasm. *Prog. Retin. Eye Res* 24, 721–753 (2005). [PubMed: 16027026]
5. Herrera E et al. , *Zic2* Patterns Binocular Vision by Specifying the Uncrossed Retinal Projection. *Cell*. 114, 545–557 (2003). [PubMed: 13678579]
6. Larsson ML, Binocular vision, the optic chiasm, and their associations with vertebrate motor behavior. *Front. Ecol. Evol* 3, 89 (2015).
7. Nakagawa S et al. , Ephrin-B regulates the Ipsilateral routing of retinal axons at the optic chiasm. *Neuron*. 25, 599–610 (2000). [PubMed: 10774728]
8. Williams SE et al. , Ephrin-B2 and EphB1 Mediate Retinal Axon Divergence at the Optic Chiasm. *Neuron*. 39, 919–935 (2003). [PubMed: 12971893]
9. Seth A et al. , *Belladonna*/(*lhx2*) is required for neural patterning and midline axon guidance in the zebrafish forebrain. *Development*. 133, 725–735 (2006). [PubMed: 16436624]
10. Heesy CP, Seeing in stereo: The ecology and evolution of primate binocular vision and stereopsis. *Evol. Anthropol* 18, 21–35 (2009).
11. Ward R, Repérant J, Hergueta S, Miceli D, Lemire M, Ipsilateral visual projections in non-etherian species: random variation in the central nervous system? *Brain Res. Rev* 20, 155–170 (1995). [PubMed: 7795654]
12. Saleeba C, Dempsey B, Le S, Goodchild A, McMullan S, A Student's Guide to Neural Circuit Tracing. *Front. Neurosci* 13, 897 (2019). [PubMed: 31507369]
13. Conte WL, Kamishina H, Reep RL, The efficacy of the fluorescent conjugates of cholera toxin subunit B for multiple retrograde tract tracing in the central nervous system. *Brain Struct. Funct* 213, 367–373 (2009). [PubMed: 19621243]
14. Luo X et al. , Three-dimensional evaluation of retinal ganglion cell axon regeneration and pathfinding in whole mouse tissue after injury. *Exp. Neurol* 247, 653–662 (2013). [PubMed: 23510761]
15. Vigouroux RJ et al. , Revisiting the role of *Dcc* in visual system development with a novel eye clearing method. *Elife*. 9, e51275 (2020). [PubMed: 32096760]
16. Hughes LC et al. , Comprehensive phylogeny of ray-finned fishes (Actinopterygii) based on transcriptomic and genomic data. *Proc. Natl. Acad. Sci. U. S. A* 115, 6249–6254 (2018). [PubMed: 29760103]
17. Amemiya CT et al. , The African coelacanth genome provides insights into tetrapod evolution. *Nature*. 496, 311–316 (2013). [PubMed: 23598338]
18. Betancur-R R et al. , Phylogenetic classification of bony fishes. *BMC Evol. Biol* 17, 162 (2017). [PubMed: 28683774]
19. Karlstrom RO et al. , Zebrafish mutations affecting retinotectal axon pathfinding. *Development*. 123, 427–38 (1996). [PubMed: 9007260]
20. Robles E, Laurell E, Baier H, The Retinal Projectome Reveals Brain-Area-Specific Visual Representations Generated by Ganglion Cell Diversity. *Curr. Biol* 24, 2085–2096 (2014). [PubMed: 25155513]

21. Voneida TJ, Sligar CM, A comparative neuroanatomic study of retinal projections in two fishes: *Astyanax hubbsi* (the blind cave fish), and *Astyanax mexicanus*. *J. Comp. Neurol* 165, 89–105 (1976). [PubMed: 1244363]
22. Fiebig E, Ebbesson SOE, Meyer DL, Afferent connections of the optic tectum in the piranha (*Serrasalmus nattereri*). *Cell Tissue Res.* 231, 55–72 (1983). [PubMed: 6850798]
23. Ebbesson SE, Ito H, Projections BR, Bilateral Retinal Projections in the Black Piranha (*Serrasalmus niger*). *Cell Tissue Res.* 213, 483–495 (1980). [PubMed: 7448850]
24. Jaillon O et al. , Genome duplication in the teleost fish *Tetraodon nigroviridis* reveals the early vertebrate proto-karyotype. *Nature.* 431, 946–957 (2004). [PubMed: 15496914]
25. Meyer DL, Fiebig E, Ebbesson SOE, A note on the reciprocal connections between the retina and the brain in the puffer fish *Tetraodon fluviatilis*. *Neurosci. Lett* 23, 111–115 (1981). [PubMed: 7254695]
26. Perez LN et al. , Eye development in the four-eyed fish *Anableps anableps*: Cranial and retinal adaptations to simultaneous aerial and aquatic vision. *Proc. R. Soc. B Biol. Sci* 284 (2017), doi:10.1098/rspb.2017.0157.
27. Butler AB, Saidel WM, Retinal Projections in the Freshwater Butterfly Fish, *Pantodon buchholzi* (*Osteoglossoidae*). *Brain. Behav. Evol* 38, 127–140 (1991). [PubMed: 1742599]
28. Lázár G, Libouban S, Szabo T, The mormyrid mesencephalon. III. Retinal projections in a weakly electric fish, *Gnathonemus petersii*. *J. Comp. Neurol* 230, 1–12 (1984). [PubMed: 6096410]
29. von der Emde G et al. , Active electrolocation in *Gnathonemus petersii*: Behaviour, sensory performance, and receptor systems. *J. Physiol. Paris* 102, 279–290 (2008). [PubMed: 18992334]
30. Braasch I, Postlethwait JH, in *Polyploidy and Genome Evolution*, Soltis P, Soltis D, Eds. (Springer Berlin Heidelberg, 2012), pp. 341–383.
31. Du K et al. , The sterlet sturgeon genome sequence and the mechanisms of segmental rediploidization. *Nat. Ecol. Evol* 4, 841–852 (2020). [PubMed: 32231327]
32. Braasch I et al. , The spotted gar genome illuminates vertebrate evolution and facilitates human-teleost comparisons. *Nat. Genet* 48, 427–437 (2016). [PubMed: 26950095]
33. Répérant J et al. , The Retinofugal Pathways in a primitive actinopterygian, the chondrosteian *Acipenser güldenstädti*. An experimental study using degeneration, radioautographic and HRP methods. *Brain Res.* 251, 1–23 (1982). [PubMed: 6184126]
34. Répérant J, Rio JP, Miceli D, Amouzou M, Peyrichoux J, The retinofugal pathways in the primitive African bony fish *Polypterus senegalus* (Cuvier, 1829). *Brain Res.* 217, 225–43 (1981). [PubMed: 7248788]
35. Northcutt RG, Butler AB, Retinofugal pathways in the longnose gar *Lepisosteus osseus* (linnaeus). *J. Comp. Neurol* 166, 1–15 (1976). [PubMed: 1262543]
36. Butler AB, Northcutt RG, Retinal Projections in the Bowfin, *Amia calva*: Cytoarchitectonic and Experimental Analysis. *Brain. Behav. Evol* 39, 169–194 (1992). [PubMed: 1511265]
37. Glenn Northcutt R, Retinal projections in the australian lungfish. *Brain Res.* 185, 85–90 (1980). [PubMed: 7353182]
38. Provis JM, Van Driel D, Billson FA, Russell P, Human fetal optic nerve: Overproduction and elimination of retinal axons during development. *J. Comp. Neurol* 238, 92–100 (1985). [PubMed: 4044906]
39. Lu Y et al. , Single-Cell Analysis of Human Retina Identifies Evolutionarily Conserved and Species-Specific Mechanisms Controlling Development. *Dev. Cell* 53, 473–491.e9 (2020). [PubMed: 32386599]
40. Hoshino A et al. , Molecular Anatomy of the Developing Human Retina. *Dev. Cell* 43, 763–779.e4 (2017). [PubMed: 29233477]
41. Kwong JMK, Caprioli J, Piri N, RNA Binding Protein with Multiple Splicing: A New Marker for Retinal Ganglion Cells. *Investig. Ophthalmology Vis. Sci* 51, 1052 (2010).
42. Wang Q, Marcucci F, Cerullo I, Mason C, *eNeuro* 3, ENEURO.0169-16.2016 (2016).
43. Toyama R, Gomez DM, Mana MD, Dawid IB, Sequence relationships and expression patterns of zebrafish *zic2* and *zic5* genes. *Gene Expr. Patterns* 4, 345–350 (2004). [PubMed: 15053986]

44. Marcucci F et al. , The Ciliary Margin Zone of the Mammalian Retina Generates Retinal Ganglion Cells. *Cell Rep.* 17, 3153–3164 (2016). [PubMed: 28009286]
45. Otteson DC, D’Costa AR, Hitchcock PF, Putative stem cells and the lineage of rod photoreceptors in the mature retina of the goldfish. *Dev. Biol* 232, 62–76 (2001). [PubMed: 11254348]
46. Fernández-Nogales M, Murcia-Belmonte V, Chen HY, Herrera E, The peripheral eye: A neurogenic area with potential to treat retinal pathologies? *Prog. Retin. Eye Res* 68 (2019), pp. 110–123. [PubMed: 30201383]
47. Braasch I et al. , A new model army: Emerging fish models to study the genomics of vertebrate Evo-Devo. *J. Exp. Zool. B. Mol. Dev. Evol* 324, 316–41 (2015). [PubMed: 25111899]
48. Long WL, Ballard WW, Normal embryonic stages of the longnose gar, *Lepisosteus osseus*. *BMC Dev. Biol* 1, 1–8 (2001). [PubMed: 11178105]
49. Lo Giudice Q et al. , Single-cell transcriptional logic of cell-fate specification and axon guidance in early-born retinal neurons. *Development.* 146, dev178103 (2019). [PubMed: 31399471]
50. García-Frigola C, Carreres MI, Vegar C, Mason CA, Herrera E, *Zic2* promotes axonal divergence at the optic chiasm midline by EphB1-dependent and -independent mechanisms. *Development.* 135, 1833–1841 (2008). [PubMed: 18417618]
51. Aruga J, Hatayama M, Comparative genomics of the *Zic* family genes. *Adv. Exp. Med. Biol* 1046, 3–26 (2018). [PubMed: 29442314]
52. Dell AL, Fried-Cassorla E, Xu H, Raper JA, cAMP-Induced Expression of *Neuropilin1* Promotes Retinal Axon Crossing in the Zebrafish Optic Chiasm. *J. Neurosci* 33, 11076–11088 (2013). [PubMed: 23825413]
53. Gebhardt C et al. , An interhemispheric neural circuit allowing binocular integration in the optic tectum. *Nat. Commun* 10, 5471 (2019). [PubMed: 31784529]
54. García-Frigola C, Herrera E, *Zic2* regulates the expression of *Sert* to modulate eye-specific refinement at the visual targets. *EMBO J.* 29, 3170–3183 (2010). [PubMed: 20676059]
55. MacIver MA, Schmitz L, Mugan U, Murphey TD, Mobley CD, Massive increase in visual range preceded the origin of terrestrial vertebrates. *Proc. Natl. Acad. Sci* 114, E2375–E2384 (2017). [PubMed: 28270619]
56. Laurent G, On the value of model diversity in neuroscience. *Nat. Rev. Neurosci* 21, 395–396 (2020). [PubMed: 32514109]
57. Hergueta S et al. , Overlapping visual fields and ipsilateral retinal projections in turtles. *Brain Res. Bull* 29, 427–433 (1992). [PubMed: 1393614]
58. Goodman CS, The likeness of being: Phylogenetically conserved molecular mechanisms of growth cone guidance. *Cell.* 78, 353–356 (1994). [PubMed: 8062381]
59. Heger P, Zheng W, Rottmann A, Panfilio KA, Wiehe T, The genetic factors of bilaterian evolution. *Elife.* 9 (2020), doi:10.7554/eLife.45530.
60. Friocourt F et al. , Recurrent *DCC* gene losses during bird evolution. *Sci. Rep* 7, 37569 (2017). [PubMed: 28240285]
61. Zelina P et al. , Signaling Switch of the Axon Guidance Receptor *Robo3* during Vertebrate Evolution. *Neuron.* 84, 1258–1272 (2014). [PubMed: 25433640]
62. Pak W, Hindges R, Lim Y-SS, Pfaff SL, O’leary DDMM, Magnitude of Binocular Vision Controlled by *Islet-2* Repression of a Genetic Program that Specifies Laterality of Retinal Axon Pathfinding. *Cell.* 119, 567–578 (2004). [PubMed: 15537545]
63. Kuwajima T, Soares CA, Sitko AA, Lefebvre V, Mason C, *SoxC* Transcription Factors Promote Contralateral Retinal Ganglion Cell Differentiation and Axon Guidance in the Mouse Visual System. *Neuron.* 93, 1110–1125.e5 (2017). [PubMed: 28215559]
64. Morenilla-Palao C et al. , A *Zic2*-regulated switch in a noncanonical *Wnt/βcatenin* pathway is essential for the formation of bilateral circuits. *Sci. Adv* 6 (2020), doi:10.1126/sciadv.aaz8797.
65. Braasch I et al. , Connectivity of vertebrate genomes: Paired-related homeobox (*Prrx*) genes in spotted gar, basal teleosts, and tetrapods. *Comp. Biochem. Physiol. Part C Toxicol. Pharmacol* 163, 24–36 (2014).
66. Marillat V et al. , Spatiotemporal expression patterns of *slit* and *robo* genes in the rat brain. *J. Comp. Neurol* 442, 130–155 (2002). [PubMed: 11754167]

67. Thisse C, Thisse B, High-resolution in situ hybridization to whole-mount zebrafish embryos. *Nat. Protoc* 3, 59–69 (2008). [PubMed: 18193022]
68. Bercier V et al. , Dynactin1 depletion leads to neuromuscular synapse instability and functional abnormalities. *Mol. Neurodegener* 14, 27 (2019). [PubMed: 31291987]
69. Edgar RC, MUSCLE: Multiple sequence alignment with high accuracy and high throughput. *Nucleic Acids Res.* 32, 1792–1797 (2004). [PubMed: 15034147]
70. Oteri F, Nadalin F, Champeimont R, Carbone A, BIS2Analyzer: A server for co-evolution analysis of conserved protein families. *Nucleic Acids Res.* 45, 307–314 (2017).
71. Santos D, Monteiro SM, Luzio A, in *Methods in Molecular Biology* 1797, 365–371 (2018). [PubMed: 29896703]

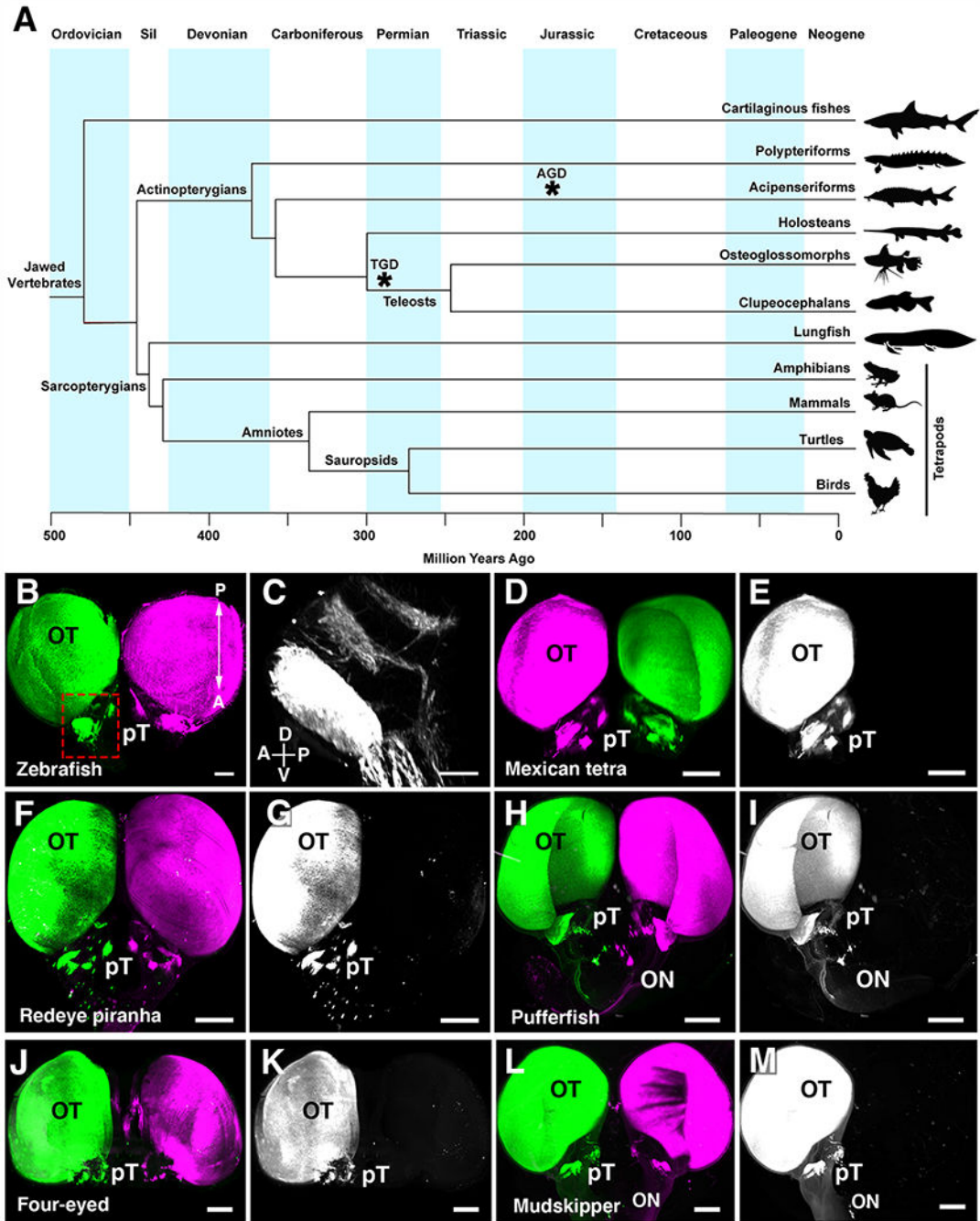


**Fig.1. Visual projections are only contralateral in clupeocephalan teleosts.**

(A) Simplified phylogenetic tree of the major groups of vertebrates. Divergence of each major group is displayed in million years. Asterisks indicate whole genome duplication events in the teleost (TGD) and sturgeon (AGD) ancestors. (B) Whole brain visualization of a juvenile zebrafish injected with an AlexaFluor-555-conjugated CTb (left eye) and AlexaFluor-647-conjugated CTb (right eye) highlighting complete contralateral projections. (C) High magnification showing pre-tectal nuclei. (D to M) 3D rendering of visual projections labelled by injecting AlexaFluor-555-conjugated CTb (left eye) and

AlexaFluor-647-conjugated CTb (right eye) followed by iDISCO whole-brain clearing and 3D imaging using light-sheet fluorescence microscopy. (D and E) Mexican tetra. (F and G) Redeye piranha. (H and I) Green-spotted pufferfish. (J and K) Four-eyed fish. (L and M) Atlantic mudskipper. In all species, visual axons only project to the brain on the contralateral side. Abbreviations: A, anterior; Cb, Cerebellum; Ctb, Cholera toxin B; D, dorsal; OB, Olfactory bulb; ON, Optic nerve; P, posterior; V, ventral; Sil, Silurian. Scale bars are 500  $\mu\text{m}$  in (B) and (D) to (M) and 200  $\mu\text{m}$  in (C).



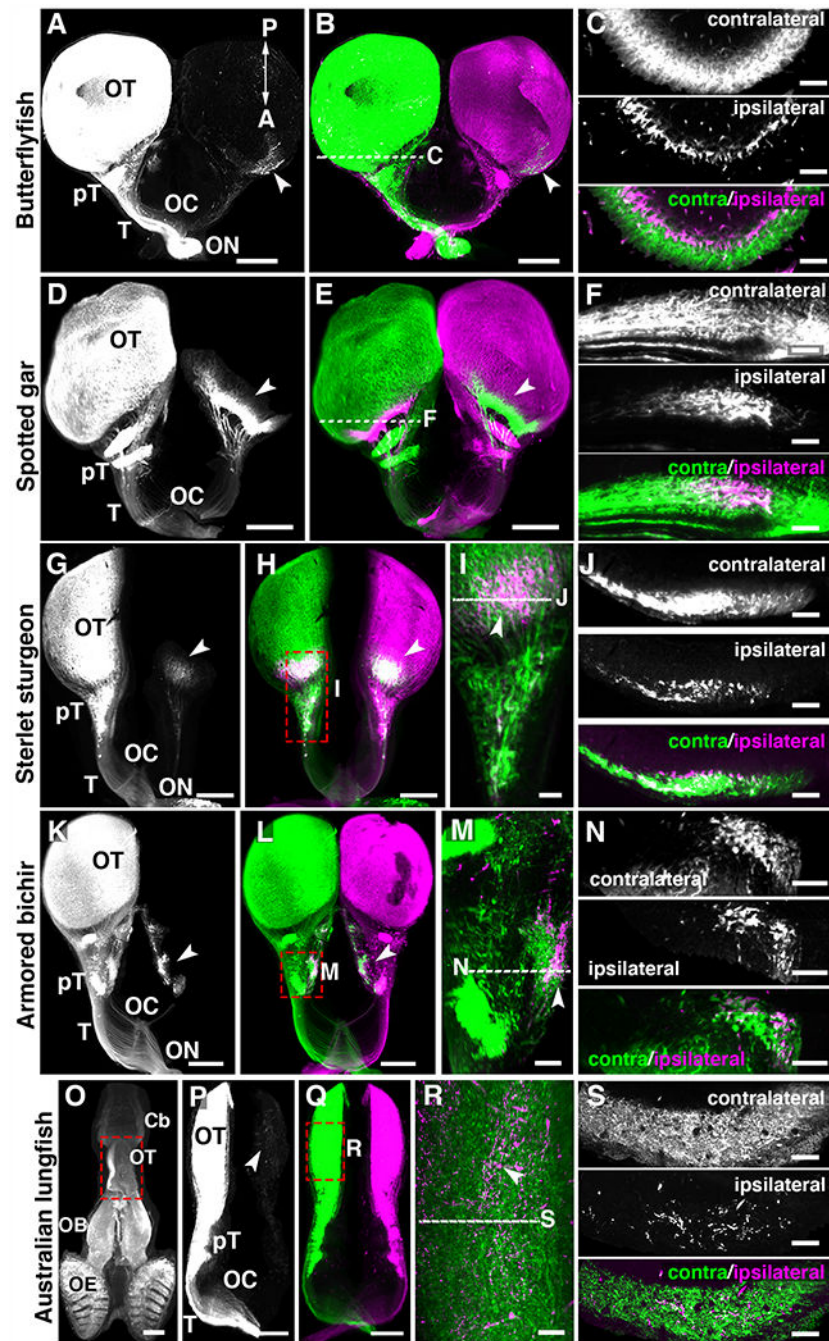


**Fig. 2. Bilateral visual projections in basal ray-finned fishes and lobe-finned fishes**  
 (A to S) 3D light-sheet fluorescence microscopy images of iDISCO+ cleared brains from fish injected into the eyes with 2 cholera toxins. The left panels show only one channel. (C, F, J, N and S) are optical sections through the brain region receiving bilateral visual inputs. (I and M and R) high magnification from whole-mount brains. (A to C) Butterflyfish. (D to F) Spotted gar. (G to J) Sterlet sturgeon. (K to N) Armored bichir. (O to S) Australian lungfish. (C, F, J and N) In all fishes, contralateral and ipsilateral projections segregate in two different optic tectum (OT) layers except in the lungfish (S) where they are intermingled

in the OT. Arrowheads indicate ipsilateral projections. Abbreviations: Cb, Cerebellum; OB, Olfactory bulb; OE, Olfactory epithelium; ON, Optic nerve; OC, Optic chiasm; pT, pretecal nuclei; T, Optic tract. Scale bars are 500  $\mu\text{m}$  in (A, B, D, E, G, H, K, L, P and Q) and 80  $\mu\text{m}$  in (C, G, K, N and S) and 100  $\mu\text{m}$  in (M, O) and 150  $\mu\text{m}$  in (I, R).

Author Manuscript

Author Manuscript

Author Manuscript

Author Manuscript

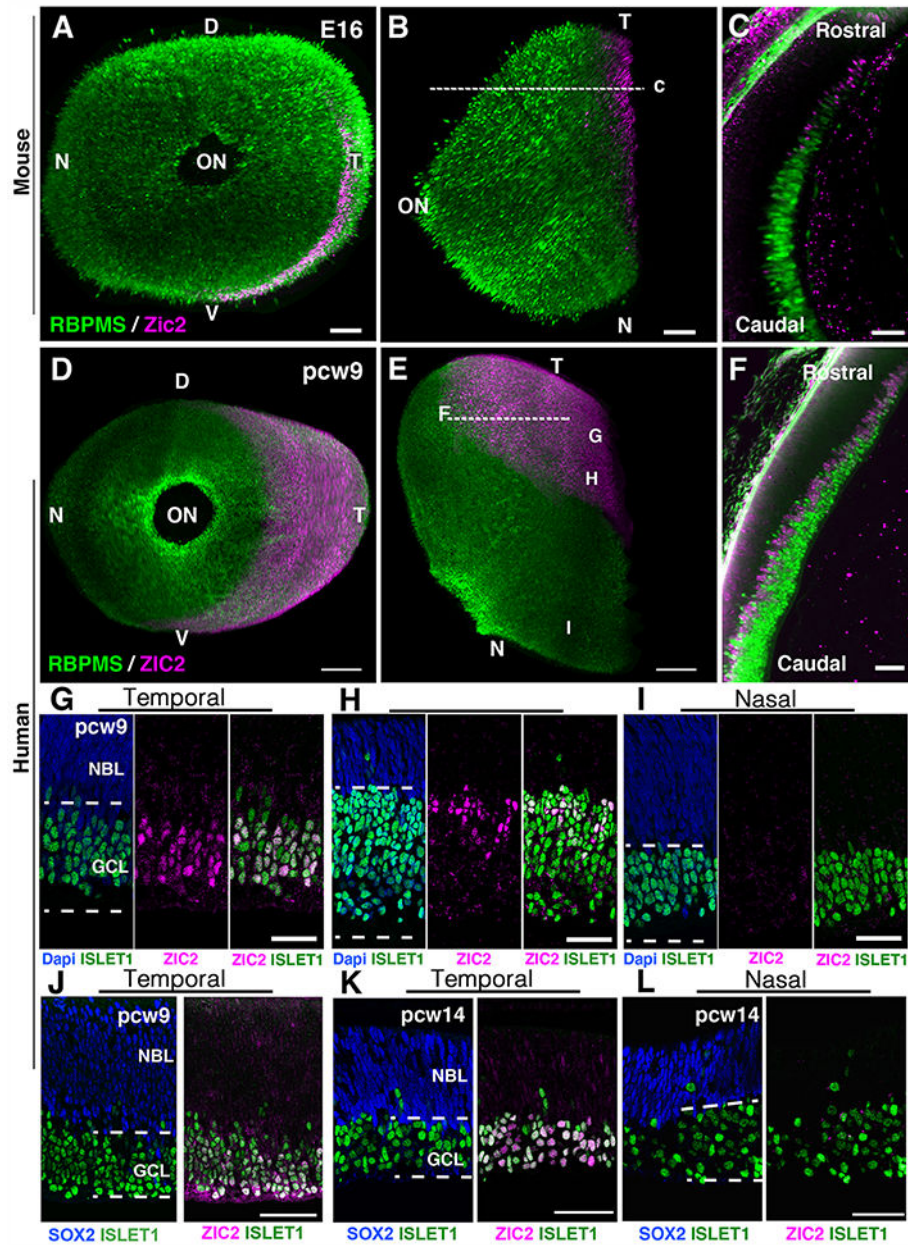


**Fig. 3. Zic2 is expressed in the temporal retina of mammal embryos**

(A to C) Whole-mount immunohistochemistry of an E16 mouse eye labeled with the pan ganglion cell marker RBPMS and the ipsilateral ganglion cell marker Zic2. (A) frontal view and (B) top view. (C) Optical section at the level indicated by the dashed line in (C). (D to F), 3D light-sheet fluorescence microscopy of pcw9 human embryonic eye cleared using EyeDISCO and labeled for RBPMS and ZIC2. (D) frontal view and (E) top view. (F) Optical section at the level indicated by the dashed line in (C). G, H, I indicate the approximate positions of images in panels G-I. (G to I) retinal cryosections of a pcw9 human embryo

eye labeled with ZIC2 and ISLET1 at 3 different levels: temporal and close to retinal outer limit (G), temporomedial (H) and nasal (I). ZIC2 cells are in the ganglion cell layer (GCL) and co-express ISLET1. They are absent from the neuroblastic layer (NBL). (J) retinal cryosection of a pcw9 human embryo eye labeled with ZIC2 and SOX2. ZIC2 is absent from the NBL which contains SOX2+ progenitors. (K and L) retinal cryosections of a pcw14 human embryo eye labeled with ZIC2, SOX2 and ISLET1. ZIC2 is only present in ISLET1+ ganglion cells in the temporal retina and absent from SOX2+ progenitors (K). Abbreviations: D, dorsal ; V, ventral ; N, nasal ; T, temporal ; ON, optic nerve. Scale bars are 70  $\mu\text{m}$  in (A and B) and 20  $\mu\text{m}$  in (C) and 300  $\mu\text{m}$  in (D and E) and 50  $\mu\text{m}$  in (F to L).



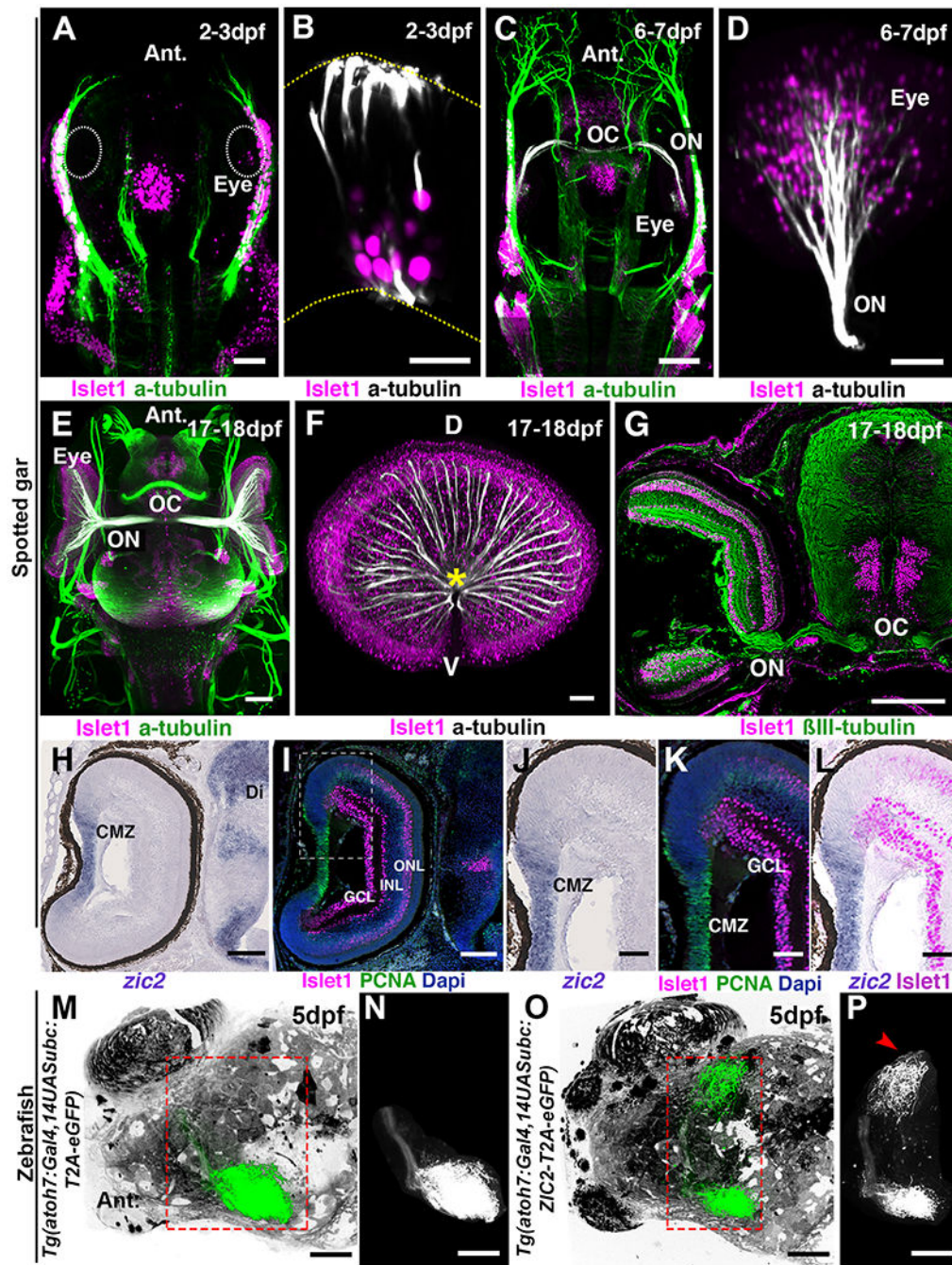


**Fig. 4. Zic2 is not expressed by ganglion cells in spotted gar and zebrafish**

(A to F) Development of the visual system in the spotted gar. All images are 3D light-sheet fluorescence microscopy images of EyeDISCO-cleared spotted gar embryos labeled with *Islet1* and acetylated Tubulin. (A and C and E) Top (dorsal) views of spotted gars at 2-3dpf (A), 6-7dpf (C), and 17-18dpf (E). (B and D and F) frontal views of whole spotted gar eyes at 2-3dpf (B), 6-7dpf (D), and 17-18dpf (F). The optic nerve (ON and asterisk) starts to form by 6-7dpf and is well developed by 17-18dpf. The optic chiasm (OC) is formed by 6-7dpf. (G) Coronal cryosection of spotted gar embryos at 17-18dpf labeled for  $\beta$ III-tubulin

and Islet1. (**H** to **K**) cryosection from 17-18dpf spotted gar eyes hybridized with *zic2* riboprobe (**H** and **J**) and labeled for proliferating cell nuclear antigen (PCNA) and Islet1 (**I**, **K** and **L**). (**J** to **L**) higher magnification of the ciliary margin zone (area framed in **I**). (**M** to **P**) 3D rendering of whole-brain viewed from the top of zebrafish injected with *Tg(ato7:Gal4,14UASubc:T2A-eGFP-pA)* (**M** and **N**) or *Tg(ato7:Gal4,14UASubc:ZIC2-T2A-eGFP-pA)* (**O** and **P**). **N** and **P** show segmented ganglion cell projections. (**P**) A large ipsilateral projection (arrowhead) is seen in the *Tg(ato7:Gal4,14UASubc:ZIC2-T2A-eGFP-pA)*-injected fish. Abbreviations: ON, Optic nerve; OC, Optic chiasm; GCL, Ganglion cell layer; INL, Inner nuclear layer; ONL, Outer nuclear layer. Scale bars are 50  $\mu\text{m}$  in (**A**, **D**, **F**, **J**, **K**, **L**, **M** to **P**) and 15  $\mu\text{m}$  in (**B**) and 80  $\mu\text{m}$  in (**C**, **H** and **I**) and 150  $\mu\text{m}$  in (**E**) and 200 $\mu\text{m}$  in (**G**).